A Coupled Active Contour Model for Myocardial Tracking in Contrast Echocardiography

Norberto Malpica[a], María Ledesma-Carbayo[a] , Andrés Santos[a], Esther Pérez[b], M.Angel García-Fernandez[b] and Manuel Desco[b]

[a]Departamento de Ingeniería Electrónica, E.T.S.I. Telecomunicación, Ciudad Universitaria s/n 28040 Madrid Spain, [b] Laboratorio de Imagen, Medicina Experimental, Hospital G. Gregorio Marañón, Madrid

Abstract. Contrast echocardiography has been proposed as an indicator of myocardial perfusion in a non-invasive way. Reperfusion curves can be obtained by destroying all the microbubbles using an ultrasound pulse with high mechanical index and acquiring images during the reperfusion process. Quantitative parameters describing the process can be obtained from the curves. To analyze the complete myocardium, we propose a method for the simultaneous segmentation and tracking of endocardium and epicardium in myocardial contrast echocardiography sequences. The model consists of two active contours, guided by optical flow estimates. The evolutions of the two contours are coupled geometrically using a novel scheme that imposes stability in wall thickness, to deal with low contrast regions in the epicardial contour. Both a closed and an open model have been designed, to account for the different acquisition views used routinely. The model has been evaluated with experimental and clinical sequences, comparing the results with manual segmentations carried out by an expert.

1 Introduction

Myocardial contrast echocardiography (MCE), due to its ability to assess microvascular integrity, has been shown to provide markers of successful reperfusion of acute myocardial infarction [1]. Viability of the myocardium is estimated by the degree of myocardial opacification following contrast injection. A method for obtaining quantitative parameters of the reperfusion process consists in destroying the contrast microbubbles with an ultrasound pulse of high energy (high mechanical index) and acquiring images continuously during the reperfusion process. It is thus possible to obtain the wash-in curve showing the refilling of the region after the destruction of the microbubbles [2]. The segmentation and time tracking of the complete myocardium in sequences acquired with a real-time acquisition would allow to analyze simultaneously wall motion and perfusion of all myocardial segments. To achieve this task, Caiani et al. [3] have proposed a method for segmenting each frame separately. The endocardium is segmented interactively in every frame of the sequence and the epicardium is obtained by dilating the edge of the endocardium a fixed width. Garcia et al. [4] have evaluated a snake model combined with an active shape model to segment four-chamber views. A previous segmentation of a high number of images is required to train the model, with the intrinsic drawback that the model allows to segment only sequences acquired in a specific view. In this work we propose the use of two active contours related by a novel coupling scheme to simultaneously segment endocardium and epicardium. A motion estimation step is incorporated to track the contours between frames.

2 Active contour model

Each active contour is represented as a discrete set of points or snaxels $\{v_1, v_2, ... v_n\}$ with $v_i = (x_i, y_i)$ [5], and the energy of the contour is defined as:

$$\varepsilon = \int_0^1 (\varepsilon_{\text{int}}(v(s)) + \varepsilon_{ima}(v(s)) + \varepsilon_{const}(v(s))) \, ds \qquad (1)$$

where ε_{int} is the internal energy, dependent on the shape of the contour, ε_{ima} is the image dependent energy, and ε_{const} represents the external constraints imposed by the user.

Two coupled active contours are used in our model, to segment the endocardium and the epicardium, respectively. The evolutions of the two curves are coupled using geometric constraints. To segment a complete sequence, only an initialization of both curves in the first frame is required. The user marks several points, and the initial contours are interpolated from these points using a B-spline curve. An evolution of the curves is then carried out to adjust the curves to image gradients. In the remaining frames, segmentation is carried out in two

stages. To compensate inter-frame displacement a first evolution is performed, based on motion estimation. A second evolution is then performed on each snake using the gradient as image energy, with distance restrictions between snakes to correct the evolution on regions of the image with low gradient.

To be able to deal with sequences acquired either in short axis views or in apical two-chamber and four-chamber views, we have designed a closed model and an open one. In the closed model the first and last points are linked together. In the open model, the first and last points of the curve only have one neighbour each. Definition of curvature and distance energies in these cases is not straightforward [5]. We set the curvature energy, $\varepsilon_{curvature} = 0$ in both ends, so the end points tend to follow their neighbours.

2.1 Internal energy

In our model, the internal energy is the addition of two terms. The first one is a curvature energy, based on the second derivative. The second term is an energy aimed at distributing snaxels uniformly along the contour. The external energy is based on the gradient of a diffusion-filtered version of the image. We have used a simple gradient based on finite differences. The energy is computed as the inverse of the gradient value.

2.2 Distance constraints

Some parts of the epicardium show a low gradient or no gradient at all due to blooming or other artefacts in the acquisition process. On these regions, an evolution of the curve based only on the gradient of the image would lead to incorrect results. The endocardium, on the contrary, is usually well depicted due to the high intensity of contrast in the cavity. We assume that the segmentation of the endocardium based only on the gradient is correct, and introduce a distance constraint, modeled as two coupling energies between the curves.

To implement this coupling, we define two distance-based energies, denoted as hard distance constraint and soft distance constraint. The hard constraint, applied to both inner and outer curves, imposes a maximum and a minimum distance between both curves, similar to that proposed by Zeng [6] for segmenting the brain cortex. When the distance between the curves is outside the allowed distance range, the energy has a very high constant value. The distance was defined based on previous manual segmentations and similar constraints proposed in the literature.

The soft constraint, applied only to the evolution of the outer curve, is a novel coupling scheme. It aims at preserving the mean distance between curves in regions with low gradients. A weighted mean distance between the curves is computed, weighting the distance of each snaxel by the value of the image gradient at that point:

$$\bar{d}_i = \frac{1}{N} \sum_{k=1}^{N} g_k \ d(v_k, C_j) \tag{2}$$

The energy of every snaxel is then computed as follows:

$$\varepsilon_{dist} = d(v_i, C_j) - \bar{d}_i \tag{3}$$

This distance energy is again weighted by the value of the gradient at every snaxel, so that the contribution of this energy is low in points with a high gradient value.

Figure 1 shows the effect of the soft constraint based on mean distance. On the left, the result of the evolution without this constraint is shown. On the right, the result with the constraint is presented. As can be observed, sections of the curve with a high gradient are not affected, while the result is corrected in sections with gradient dropouts.

2.3 Motion energy

To take advantage of temporal information and make the segmentation more efficient, we define a motion energy based on inter-frame displacement estimation. As reported in [7] we tested several optical flow methods to track regions of interests in contrast echocardiography sequences. The best results were obtained with the method proposed by Lucas and Kanade [8].

A multiscale version of the algorithm was designed, using a four-level Gaussian pyramid to capture large displacements without a major increase in computational load. The displacement is first computed at the lowest resolution. The algorithm is then applied at higher levels, starting from the displacements obtained in the previous level.

Once we have obtained a displacement for every control point, the energy at each point of the neighbourhood is defined as the distance in pixels to the displaced point. Internal energies are also taken into account. The compete model is thus:

$$\varepsilon = \int_0^1 (\alpha \varepsilon_{mot}(v(s)) + \beta \varepsilon_{int}(v(s)) + \gamma \varepsilon_{const}(v(s))) \, ds \tag{4}$$

where ε_{mot} represents motion energy. In all experiments, the parameters used were $\alpha = 1.0$, $\beta = 0.6$, $\gamma = 0.8$.

Fig 1. Result of curve evolution without distance constraints (left) and including the constraints (right)

3 Experiments and Results

For evaluating the closed model, six short axis sequences acquired from pigs during experimental surgery were used, with a total of 221 images. The open model was tested on 181 images from 6 sequences, obtained in clinical routine from 6 different patients. Three of the sequences were two chamber views and three were four chamber views. Images were acquired with Contrast Pulse Sequencing (CPS), a real-time acquisition method with an Acuson Sequoia (Acuson-Siemens) scanner. All the images were manually segmented by an expert observer, and by the automatic model. To compare both segmentations, two parameters were obtained: mean distance between curves and Hausdorff distance (maximum distance from a point of a curve to the other curve). For the close model, the degree of overlap between segmented surfaces was also computed. The results are summarized in table 1 (closed model) and table 2 (open model). Examples of the segmentation of two frames are shown in figure 2.

The proposed algorithm achieved good results both in endocardium and epicardium. Differences with manual segmentation results are larger in the epicardium, due to the lack of information in that part of the image. Results are similar to those presented by [4], but their model required a priori training by manual segmentation of a high number of images.

	Degree of overlap	Mean distance (mm)	Hausdorff distance (mm)
Endocardium	97.7 % ± 0.12 %	1.46 ± 0.70	2.34 ± 1.54
Epicardium	94.5 % ± 2.11 %	1.87 ± 0.63	3.21 ± 1.97

Table 1. Comparison between manual and automatic segmentation results for the closed model

	Mean distance (mm)	Hausdorff distance (mm)
Endocardium	1.33 ± 0.69	3.23 ± 2.01
Epicardium	1.75 ± 0.82	3.91 ± 2.52

Table 2. Comparison between manual and automatic segmentation results for the open model

(a) (b) (c) (d)
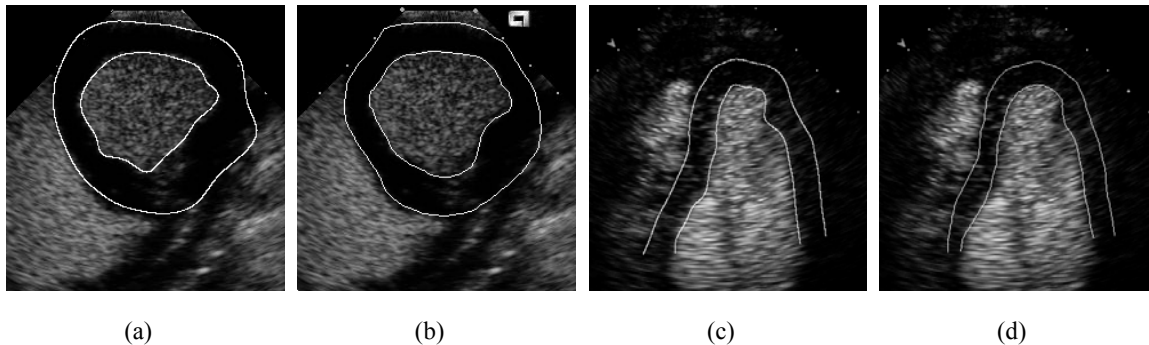
Figure 2. Comparison between automatic and manual segmentations. Automatic (a) and manual segmentation (b) of a short axis frame. Automatic (c) and manual segmentation (d) of a four chamber view frame.,

4 Discussion and Conclusion

We have proposed a model consisting of two coupled active contours. Our model is automatic, except for the definition of the myocardium by the user in the first image. The advantage with respect to previous proposals is that it does not require a training of the model, avoiding the need of time-consuming expert interaction and making it more general, allowing to segment sequences acquired in different views. Another advantage is the inclusion of an optical flow stage to compensate for motion between frames, which allows for an efficient tracking even in sequences acquired with a low frame rate. When there is no other information (lack of image contrast), the method makes the assumption of uniform myocardial thickness in each frame. This may not be correct in some pathological cases, in which some segments may have a reduced thickness. No other a priori information is needed.

References

1. M. A. Vannan and B. Kuersten, "Imaging techniques for myocardial contrast echocardiography," *European Journal of Echocardiography*, vol. 1, pp. 224-226, 2000.
2. K. Wei, A. R. Jayaweera, S. Firoozan, A. Linka, D. M. Skyba, and S. Kaul, "Quantification of myocardial blood flow with ultrasound-induced destruction of microbubbles administered as a constant venous infusion," *Circulation*, vol. 97, pp. 473-83, 1998.
3. E. G. Caiani, R. M. Lang, S. Caslini, K. A. Collins, C. E. Korcarz, and V. Mor-Avi, "Quantification of regional myocardial perfusion using semiautomated translation-free analysis of contrast-enhanced power modulation images," *Journal of the American Society of Echocardiography*, vol. 16, pp. 116-23, 2003.
4. J. Garcia, D. Rotger, P. Radeva, F. Carreras, and R. Leta, "Contrast Echography Segmentation and Tracking by a Trained Deformable Model," *Proceedings of Computers in Cardiology*, Thessaloniki, 30:173-177 Thessaloniki Greece, 2003.
5. S. Lobregt and M. A. Viergever, "A discrete dynamic contour model," *IEEE Transactions on Medical Imaging*, vol. 14, pp. 12-24, 1995.
6. X. Zeng, L. H. Staib, R. T. Schultz, and J. S. Duncan, "Segmentation and measurement of the cortex from 3-D MR images using coupled-surfaces propagation," *IEEE Transactions on Medical Imaging*, vol. 18, pp. 927-37, 1999.
7. N. Malpica, A. Santos, M. A. Zuluaga, M. J. Ledesma, E. Pérez, M. A. García-Fernández, and M. Desco, "Tracking of Regions-of-Interest in Myocardial Contrast Echocardiography," *Ultrasound in Medicine and Biology*, vol. 30, pp. 303-309, 2004.
8. B. Lucas and T. Kanade, "An iterative image registration technique with an application to stereo vision," *Proceedings DARPA IU Workshop*, 1981.